



HAL
open science

Identification of Vertical Profiles of Reflectivity for Correction of Volumetric Radar Data Using Rainfall Classification

Pierre-Emmanuel Kirstetter, Hervé Andrieu, Guy Delrieu, Brice Boudevillain

► **To cite this version:**

Pierre-Emmanuel Kirstetter, Hervé Andrieu, Guy Delrieu, Brice Boudevillain. Identification of Vertical Profiles of Reflectivity for Correction of Volumetric Radar Data Using Rainfall Classification. *Journal of Applied Meteorology and Climatology*, 2010, 49 (10), pp.2167-2180. 10.1175/2010JAMC2369.1 . insu-00564401

HAL Id: insu-00564401

<https://insu.hal.science/insu-00564401>

Submitted on 6 Dec 2020

HAL is a multi-disciplinary open access archive for the deposit and dissemination of scientific research documents, whether they are published or not. The documents may come from teaching and research institutions in France or abroad, or from public or private research centers.

L'archive ouverte pluridisciplinaire **HAL**, est destinée au dépôt et à la diffusion de documents scientifiques de niveau recherche, publiés ou non, émanant des établissements d'enseignement et de recherche français ou étrangers, des laboratoires publics ou privés.

NOTES AND CORRESPONDENCE

Identification of Vertical Profiles of Reflectivity for Correction of Volumetric Radar Data Using Rainfall Classification

PIERRE-EMMANUEL KIRSTETTER

Laboratoire Atmosphères, Milieux, Observations Spatiales, Vélizy, France

HERVÉ ANDRIEU

Division Eau, Laboratoire Central des Ponts et Chaussées, Bouguenais, France

GUY DELRIEU AND BRICE BOUDEVILLAIN

Laboratoire d'étude des Transferts en Hydrologie et Environnement, Grenoble, France

(Manuscript received 11 August 2009, in final form 27 May 2010)

ABSTRACT

Nonuniform beam filling associated with the vertical variation of atmospheric reflectivity is an important source of error in the estimation of rainfall rates by radar. It is, however, possible to correct for this error if the vertical profile of reflectivity (VPR) is known. This paper presents a method for identifying VPRs from volumetric radar data. The method aims at improving an existing algorithm based on the analysis of ratios of radar measurements at multiple elevation angles. By adding a rainfall classification procedure defining more homogeneous precipitation patterns, the issue of VPR homogeneity is specifically addressed. The method is assessed using the dataset from a volume-scanning strategy for radar quantitative precipitation estimation designed in 2002 for the Bollène radar (France). The identified VPR is more representative of the rain field than are other estimated VPRs. It has also a positive impact on radar data processing for precipitation estimation: while scatter remains unchanged, an overall bias reduction at all time steps is noticed (up to 6% for all events) whereas performance varies with type of events considered (mesoscale convective systems, cold fronts, or shallow convection) according to the radar-observation conditions. This is attributed to the better processing of spatial variations of the vertical profile of reflectivity for the stratiform regions. However, adaptation of the VPR identification in the difficult radar measurement context in mountainous areas and to the rainfall classification procedure proved challenging because of data fluctuations.

1. Introduction

The vertical variation of reflectivity in the radar beam is a dominant source of error in the measurement of rainfall by radar. Its correction requires prior determination of the vertical profile of reflectivity (VPR). Various approaches have been proposed to determine the VPR: 1) climatological averages of measured reflectivities as a function of the altitude (Joss and Lee 1995), 2) characterization of a synthetic VPR by estimation of a limited

number of parameters such as the brightband altitude and peak, the reflectivity vertical gradient beyond and above the melting layer, and so on (Kitchen et al. 1994), and 3) retrieval of the VPR by filtering the beam-sampling effects from the comparison of radar data at different distances and different altitudes (Andrieu and Creutin 1995; Andrieu et al. 1995; Seo et al. 2000). These studies have inspired correction methods that are used operationally (Harrison et al. 2000; Germann et al. 2006; Tabary 2007; Tabary et al. 2007). Over the last decade, volumetric sampling of the atmosphere by radar has become the standard operational protocol for weather radars, leading the way to improved VPR identification methods (Vignal et al. 1999; Marzano et al. 2004; Germann and Joss 2002) and detection of the bright band, an important component

Corresponding author address: Dr. Pierre-Emmanuel Kirstetter, LATMOS, UMR 8190 (UVSQ, CNRS, PARIS VI), 11, boulevard d'Alembert, 78280 Guyancourt, France.
E-mail: pierre-emmanuel.kirstetter@latmos.ipsl.fr

of the VPR (Sanchez-Diezma et al. 2000; Gourley and Calvert 2003; Zhang et al. 2008). Nevertheless, the resulting corrections are not yet fully satisfactory for several reasons listed by Bellon et al. (2005, 2007), who emphasize the influence of VPR variability. This assessment is confirmed by Berne et al. (2004), who show that the differences between rain gauge and radar measurements at short time steps are largely explained by VPR fluctuations.

Thus, progress is needed in the correction of radar data for VPR variability. Three approaches can be investigated: 1) the use of polarimetric parameters to better characterize hydrometeors (Matrosov et al. 2007), 2) coupling of radar data analysis with the modeling of the vertical variations of reflectivity, by means of detailed microphysical models (Zawadzki et al. 2005) or more simple models (Boudevillain and Andrieu 2003), and 3) an in-depth analysis of volumetric radar data by means of existing methods. This note examines this last alternative and evaluates the ability of the VPR identification method proposed by Vignal et al. (1999) to cope with the spatial variations of the VPR and different rain types. It complements a recently published article (Delrieu et al. 2009) that describes a developmental radar quantitative precipitation estimation (QPE) processing system called Traitements Régionalisés et Adaptatifs de Données Radar pour l'Hydrologie (Regionalized and Adaptive Radar Data Processing for Hydrological Applications), or TRADHy.

The TRADHy strategy, focused on radar QPE from noncoherent volume-scanning data, consists of four steps: 1) a preprocessing step aimed at checking radar calibration stability, determining the detection domain, and characterizing dry-weather clutter; 2) identification during the course of a rain event to dynamically determine clutter, on the one hand, and rain types (convective, stratiform, or undetermined) and the corresponding VPRs on the other; 3) corrections for both clutter and screening effects, along with a projection of measured reflectivities onto the ground level using the identified rain-typed VPRs—the VPR effects, together with the screening effects, are corrected for using high-resolution terrain data of the area, a three-dimensional model of the radar beam propagation assuming beam refraction of standard atmospheric conditions and accounting for the earth curvature effect, and an estimation of the VPR (Pellarin et al. 2002); and 4) estimation of rainfall at ground level by considering a reflectivity–rain rate conversion that may depend on rain type.

Regarding the identification of the rain types, variants of the algorithms by Steiner et al. (1995) for identifying convective cells and Sanchez-Diezma et al. (2000) for detecting the bright band (indicative of stratiform rainfall) are implemented to determine convective and stratiform

rainfall, respectively. A decision tree was elaborated for the synergy of these two algorithms. They were found to be very effective at short range (less than about 80 km) and, because of radar sampling limitations, much less satisfactory as range increases. The brightband altitude identification proved in particular to be very sensitive to radar sampling strategy and radar range. VPR identification is performed using the algorithm presented in this note. It was found to be useful to refine the rain classification using the identified VPRs, resulting in a coupled identification of the rain types and the corresponding VPRs. In the correction scheme, the profile determined for all rainy pixels (referred to as “global” VPR hereinafter) is used for the “undetermined” area.

This note focuses on VPR identification using rain types (convective or stratiform) and is organized as follows. Section 2 reviews the VPR identification method. Section 3 introduces the case study, and section 4 details the application conditions of the VPR identification method for time-varying geographical domains. Section 5 proposes various assessments of the method, and section 6 concludes the paper.

2. The VPR identification method

We define the VPR as a function describing the evolution of the *mean* equivalent reflectivity (i.e., the sixth-order moment of the rain drop size distribution, assumed to be in liquid phase) as a function of the altitude, over a given space–time domain. This definition generates a number of comments: 1) The VPR function is representative of the variability of the reflectivity field from a vertical perspective over the domain. Rainfall heterogeneity results from complex microphysical processes, and variability around the VPR function is likely to be strong. 2) One practical problem in VPR estimation lies in the fact that measured reflectivity values integrate the VPR over a given altitude range. Using measured reflectivities produces increasingly smoother VPR functions as the radar range increases. 3) In accordance with Andrieu and Creutin (1995), we are actually considering a normalized function for the VPR. In so doing, it becomes implicitly assumed that reflectivity factor $Z(x, h)$ at location x and altitude h can be expressed as the product of its value at ground level and the VPR value at the considered altitude:

$$Z(x, h) = Z(x, h_0)z_D(h), \quad (1)$$

where $Z(x, h_0)$ is the reflectivity factor at the reference altitude h_0 (usually ground level). The function $z_D(h)$ is called the VPR and is assumed to be homogeneous over the considered domain D .

We define the various types of VPRs being discussed in this paper. Note that their space–time characteristics

differ from those of the “true” VPR retrieved quasi instantaneously on very small domains by vertically pointing radar because they are representative of much larger domains and time integration periods. They differ from each other by the space–time domain D upon which the VPR is retrieved (details are given in section 4a) and to what extent the beam effects are corrected in the VPR identification:

- 1) the *apparent* VPR (which is also the a priori VPR) is computed by averaging reflectivities conditioned by rain types measured up to ~ 60 km from the radar and is influenced by smoothing radar sampling effects (details are given in section 4b);
- 2) the *identified* VPR is corrected for the radar sampling effects and is retrieved from typed reflectivities measured up to ~ 120 km from the radar, which corresponds to the window of the Cévennes–Vivarais Mediterranean Hydrometeorological Observatory (CVMHO) pilot site (see Delrieu et al. 2005, 2009) where dense rain gauge networks are available.

The method developed hereinafter addresses specifically the issue of VPR homogeneity by performing the identification over areas of homogeneous rain types. Relative to previous work, we expect to increase the representativity of the VPRs if computed on domains of consistent microphysical processes. The radar sampling issue is addressed with the correction method initially proposed by Andrieu and Creutin (1995) and Andrieu et al. (1995) and further developed by Vignal et al. (1999). It is adapted here to the case of time-varying geographical regions (Kirstetter 2008).

We recall that the method applies to a ratio of radar measurements linked to the VPR by a nonlinear model of the radar sampling:

$$q_z(x, A_{\text{ref}}, A_i) = \frac{\bar{Z}(x, A_i)}{\bar{Z}(x, A_{\text{ref}})} = \frac{\int_{H^-(\theta_0, A_i)}^{H^+(\theta_0, A_i)} f^4(\theta_0, h) z_D(h) dh}{\int_{H^-(\theta_0, A_{\text{ref}})}^{H^+(\theta_0, A_{\text{ref}})} f^4(\theta_0, h) z_D(h) dh}, \quad (2)$$

where q_z is the reflectivity ratio, $f^4(\theta_0, h)$ is the two-way normalized power-gain function of the radar antenna at altitude h , θ_0 is the 3-dB beamwidth, and A_{ref} and A_i are the reference (often the lowest) and a higher elevation angle, respectively. The ratios are computed at the same location and at different elevation angles as a function of distance. They can then be used to filter the horizontal variability of radar reflectivity factor at ground level. The function q_z may be interpreted as the signature of the

VPR z_D modified by both the beam geometry and the use of a ratio. If the VPR is discretized into n_z vertical components of incremental height D_h regrouped in the vector $\mathbf{Z}(z_1, \dots, z_{n_z})$, then Eq. (2) becomes

$$q_{i,j} = \frac{\sum_{k=1}^{k=n_z} \phi_k(x_j, A_i) z_k}{\sum_{k=1}^{k=n_z} \phi_k(x_j, A_{\text{ref}}) z_k}, \quad (3)$$

where the coefficient ϕ_k represents the contribution of the received power associated with the k th VPR component at distance x_j for the elevation angle A_i .

The method identifies the VPR that demonstrates the best compromise with respect to the maximum likelihood between 1) reconstituting the experimental values of ratios [according to the theoretical model of the radar sampling defined by Eq. (2)] and 2) staying close to an a priori guess. The apparent VPR thus serves as this a priori guess. The identification is performed by a classical algorithm (Menke 1989) that consists of minimizing the following expression:

$$\begin{aligned} \varphi(\mathbf{z}, \mathbf{q}) &= (\mathbf{z} - \mathbf{z}_0)^T \mathbf{C}_z^{-1} (\mathbf{z} - \mathbf{z}_0) + (\mathbf{q} - \mathbf{q}_0)^T \mathbf{C}_q^{-1} (\mathbf{q} - \mathbf{q}_0) \\ \mathbf{q} &= m(\mathbf{z}) \end{aligned}, \quad (4)$$

where φ is a likelihood function, m is the theoretical model relating the vector of ratios \mathbf{q} to the vector of the discretized VPR \mathbf{z} , \mathbf{q}_0 denotes the vector of observed ratios, \mathbf{z}_0 is the a priori VPR, and \mathbf{C}_q and \mathbf{C}_z are the covariance matrices of ratios \mathbf{q} and VPR components \mathbf{z} , respectively (the superscripts -1 and T stand for “inverse” and “transpose”, respectively). The covariance matrices reflect the respective confidence allocated to the a priori VPR and the ratios and their specification allows establishing a balance between data (i.e., ratios) and a priori information. The statistical distributions of both \mathbf{q} and \mathbf{z} are assumed to be Gaussian. Menke (1989) demonstrates that the solution vector \mathbf{z}' satisfies

$$\begin{aligned} \mathbf{z}' &= \mathbf{z}_0 + \mathbf{C}_z \mathbf{M}^T (\mathbf{M}^T \mathbf{C}_z \mathbf{M} + \mathbf{C}_q)^{-1} \\ &\quad \times [\mathbf{q}_0 - m(\mathbf{z}') + \mathbf{M}(\mathbf{z}' - \mathbf{z}_0)], \end{aligned} \quad (5)$$

where \mathbf{M} is the matrix of partial derivatives of the model m . If the model m is nonlinear, then Eq. (5) can be solved using an iterative method. The algorithm modifies the a priori VPR to derive the identified VPR in a series of converging steps.

The method was initially developed to derive information on the VPR from radar data at two elevations angles (Andrieu and Creutin 1995; Andrieu et al. 1995).

It was extended to volumetric radar data by Vignal et al. (1999). The enhanced volumetric sampling of the atmosphere [e.g., 10 plan position indicators (PPI) in the paper referred to above] made it possible to estimate “local” VPRs at the hourly time step for *fixed* geographical domains of typically 15° of azimuth extension and 10–30 km of radial extension, depending on the radar range. This work and two additional assessment exercises conducted within the Swiss and U.S. radar networks (Vignal et al. 2000; Vignal and Krajewski 2001) proved that VPR correction based on such local VPRs improves slightly but systematically the rainfall estimation at ground level relative to no VPR correction and to correction based on apparent VPRs [the VPRs estimated by averaging measured reflectivities in the vicinity of the radar site, using, for instance, the method proposed by Germann and Joss (2002)]. As compared with the fixed geographical domains considered in these early studies, space–time-varying geographical domains derived from the rain classification algorithm may make it possible to improve VPR identification.

3. Case study

A detailed description of the Bollène 2002 experiment can be found in Delrieu et al. (2009). This experiment was designed to evaluate the benefits of a radar volume-scanning strategy for radar QPE in mountainous regions and served to establish the TRADHy developmental software. During the experiment, the Bollène radar performed 3 PPIs at angles of 0.8°, 1.2°, and 1.8° at an antenna rotation rate of 10° s⁻¹, complemented by two sets of 5 PPIs, alternated every 5 min at an antenna rotation rate of 15° s⁻¹, allowing a good sampling of the atmosphere at 10-min intervals (see Table 2 in Delrieu et al. 2009). The radar reflectivity data are available for each 1 × 1 km² Cartesian mesh of each PPI.

Five intense rain events were sampled during the Bollène 2002 experiment, including the catastrophic mesoscale convective system of 8–9 September 2002 (Delrieu et al. 2005; Bonnifait et al. 2009), two frontal systems (21 October and 21 November 2002), and two shallow convective events triggered by the orography of the Cévennes region (24 November and 10–13 December 2002). Table 3 in Delrieu et al. (2009) summarizes the main characteristics of the five rain events selected for this study; these events cover a broad array of Mediterranean rain systems and span a total duration of 176 h. To illustrate the application conditions of the VPR identification in section 4, we will be using 1 h of radar data, characterized by a marked spatial heterogeneity, collected during the 8–9 September 2002 case. For the assessment of the method in section 5, the entire radar dataset will be used

together with the rain gauge data available from the CVMHO networks (Delrieu et al. 2009).

4. Application conditions of VPR identification

The VPR identification method is sensitive to the choice of the a priori VPR z_0 retained to initialize the algorithm and to the error structure of the data (reflectivity ratios). As stated by Vignal et al. (1999), the VPR homogeneity and the rainfall intermittency on the identification domain affect the calculation and the representativeness of the ratios and the retrieved VPR. Thus, the application of the VPR identification method requires careful preparation to 1) satisfy as well as possible the assumption of VPR homogeneity, 2) define the a priori VPR and its level of confidence, and 3) choose the data and their level of confidence. These three points are examined in the following paragraphs.

a. VPR identification domain

Figure 1 displays the rain-partitioning results in the study domain at two time steps (0100 and 0200 UTC) on 9 September 2002. The rain classification detects convective, stratiform, and transition (or undetermined) rainfall. As noted in Delrieu et al. (2009), the convective algorithm is found to be satisfactory while the stratiform algorithm fails at detecting the entire stratiform trail of the mesoscale convective system (MCS; north part of the images) as a result of the radar sampling limitations, especially at ranges that are greater than 100 km. However, we work hereinafter with this version of the rain separation, which will be the subject of further improvements in the future. Figure 2 displays corresponding quantiles of the probability density functions of hourly apparent VPRs (0100–0200 UTC) for all of the rainy pixels and for the convective and stratiform rainy pixels. Various range intervals are considered: 20–30, 40–50, and 60–70 km. The convective and stratiform median profiles are very different, which confirms that rain separation provides an effective way of sorting. It may be assumed that VPR populations are more homogeneous within each rain type. This result justifies the use of rainfall classification for VPR identification. Two variabilities can be distinguished by considering the range-dependent distributions. The variability of VPR with distance is caused by radar sampling; a residual variability appears whatever the range is. The apparent VPR degrades with range, and it clearly appears that the bright band of stratiform VPRs becomes thicker and less intense because of the beam widening. The stratiform distribution at range interval 60–70 km is so degraded that it looks like the convective distribution. This could be related to the range limitations of the brightband identification and of the rain classification,

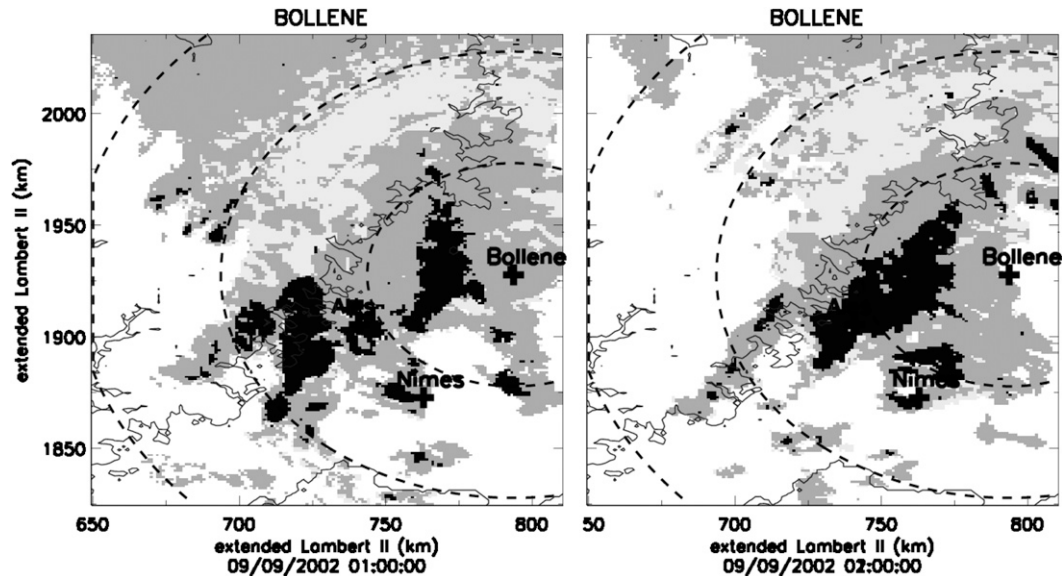


FIG. 1. Results of rain separation in the case of the MCS observed at (left) 0100 and (right) 0200 UTC 9 Sep 2002: (black: convective rainfall; light gray: stratiform rainfall; dark gray: undetermined). Range markers are displayed at 50-km intervals.

and it emphasizes the need to identify the VPR to filter the beam effects as much as possible.

As a consequence, a representative VPR is to be identified for each rain-typed zone and each time step. Germann and Joss (2002) recommend matching spatial and temporal scales (2 h and 100 km for their case). Extensive analysis of the VPR distributions indicates that the statistical distributions of both the convective pixels and the stratiform pixels were very comparable in terms of quantiles at the 5- and 60-min time steps, the latter being smoother and more regular. Although in-depth analysis of the convective and stratiform patterns may be useful to precisely define such relevant space–time scales, our choice for VPR identification is to consider the space–time domains defined by the rain regions classified in a given rain type over the 1-h period preceding the time of interest. We therefore assume that the VPR remains spatially homogeneous at an hourly time step inside each type of rain zone. A difficulty comes from the fact that these rain zones move from one time step to the next (Fig. 1), which makes it impossible to consider fixed geographical domains. Now we have to define the a priori VPR and the data for the selected domain.

b. Choice of the a priori VPR

VPR identification is initialized by an a priori VPR. Our confidence in this a priori VPR is quantified by the error covariance. The adopted a priori VPR is the apparent VPR; it was inspired by Germann and Joss (2002), who derived an average VPR from measured reflectivities not too far from the radar (e.g., 70 km) to

limit the beam-smoothing influence. Hereinafter, the domains of the apparent VPRs are similar to the identified VPR (an hourly time step inside each type of rain zone) but on a closer vicinity to the radar site (typically 60 km). This a priori VPR, detailed in Delrieu et al. (2009), may be seen as a range-weighted average VPR. It takes into account the radar sampling properties and gives a more important weight as the radar measurements are closer to the radar site. The weights are computed from radar sampling modeling that considers a radar measurement performed at an altitude h to represent the VPR integrated over an altitude range determined by the 3-dB beamwidth using a Gaussian model for the antenna diagram. The VPR thus calculated remains, however, influenced by beam smoothing as the radar range increases and in the presence of strong vertical reflectivity gradients (stratiform VPR). The a priori VPRs are illustrated in Fig. 3. Note that the convective and stratiform apparent VPRs are very distinct, which confirms the efficiency of the rainfall classification. In accordance with simulations of beamwidth-smoothing effects versus range (Sanchez-Diezma et al. 2000; Vignal et al. 1999), we may expect the true bright band of the stratiform VPR to be finer and higher than the bright band of the apparent VPR. The global apparent VPR is not very different from the convective one, indicating the dominant weight of the convective pixels within the 60-km range (Fig. 1).

c. Data

The observed data are the reflectivity ratios calculated up to 120 km from the radar using the following expression:

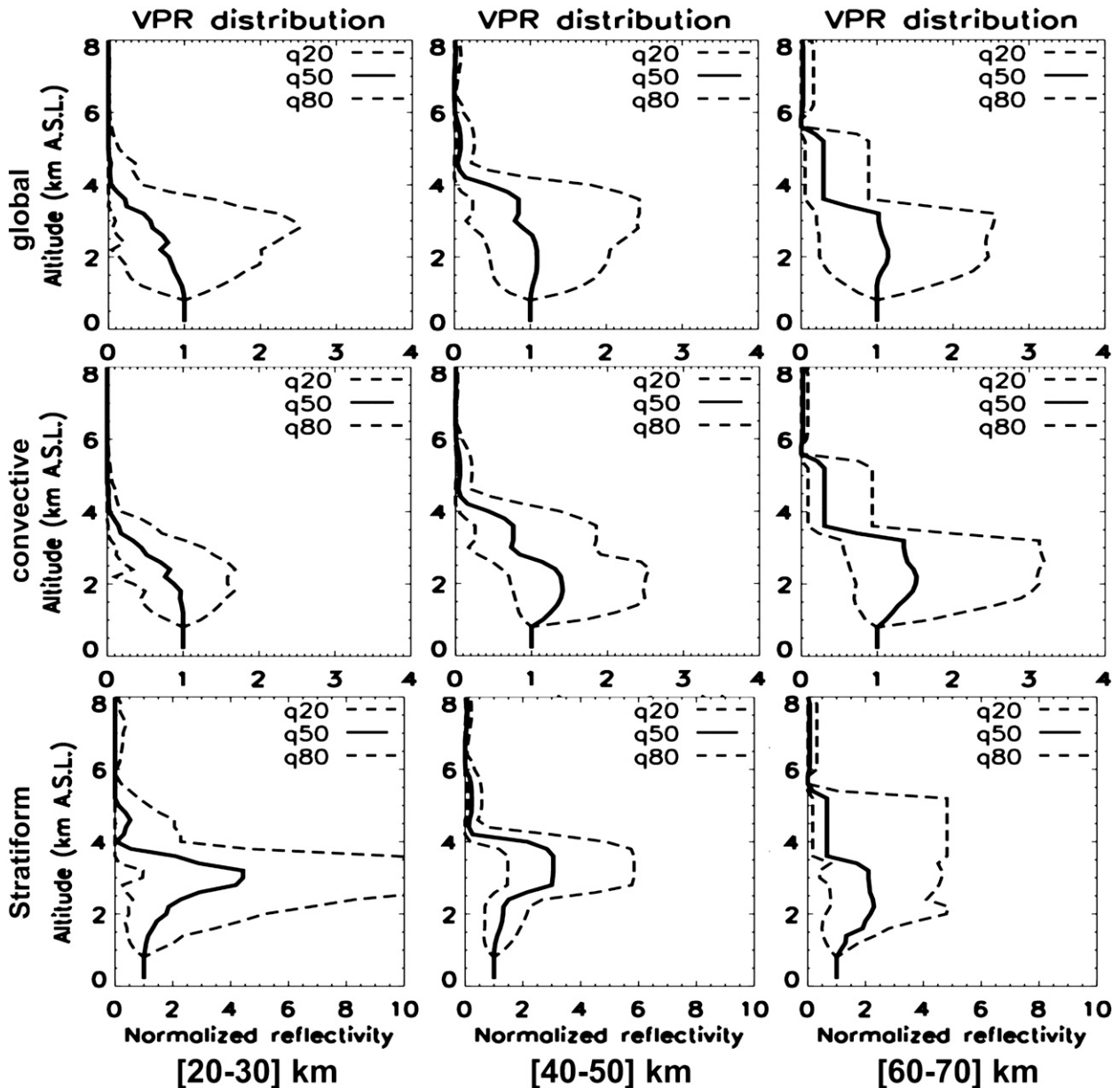


FIG. 2. Statistical distributions of the VPRs between 0100 and 0200 UTC 9 Sep 2002. The 20%, 50%, and 80% quantiles of the normalized reflectivity factor distributions are displayed (top) for all rainy pixels and for (middle) convective and (bottom) stratiform pixels. The median profile is represented by the plain curves. The reflectivity factor at a given altitude is normalized by the average reflectivity factor value in the first kilometer above sea level. The profiles are established using reflectivity factor measurements within the (left) 20–30-, (center) 40–50-, and (right) 60–70-km ranges. Note that the range abscissa is 0–4 for global and convective types and 0–10 for the stratiform type.

$$q(r, A_i, A_{\text{ref}}) = \frac{\sum_{j=1}^{N(r, A_i, A_{\text{ref}})} Z_{m,j}(r, A_i)}{\sum_{j=1}^{N(r, A_i, A_{\text{ref}})} Z_{m,j}(r, A_{\text{ref}})} \quad (6)$$

The values $Z_{m,j}(r, A_i)$ and $Z_{m,j}(r, A_{\text{ref}})$ ($\text{mm}^6 \text{m}^{-3}$) are measured reflectivities (subscript m) at a given time and location (symbolized by subscript j) observed at a distance r and at upper and reference elevation angles A_i and A_{ref} , respectively. Although the radar data are corrected for ground clutter and partial beam blocking

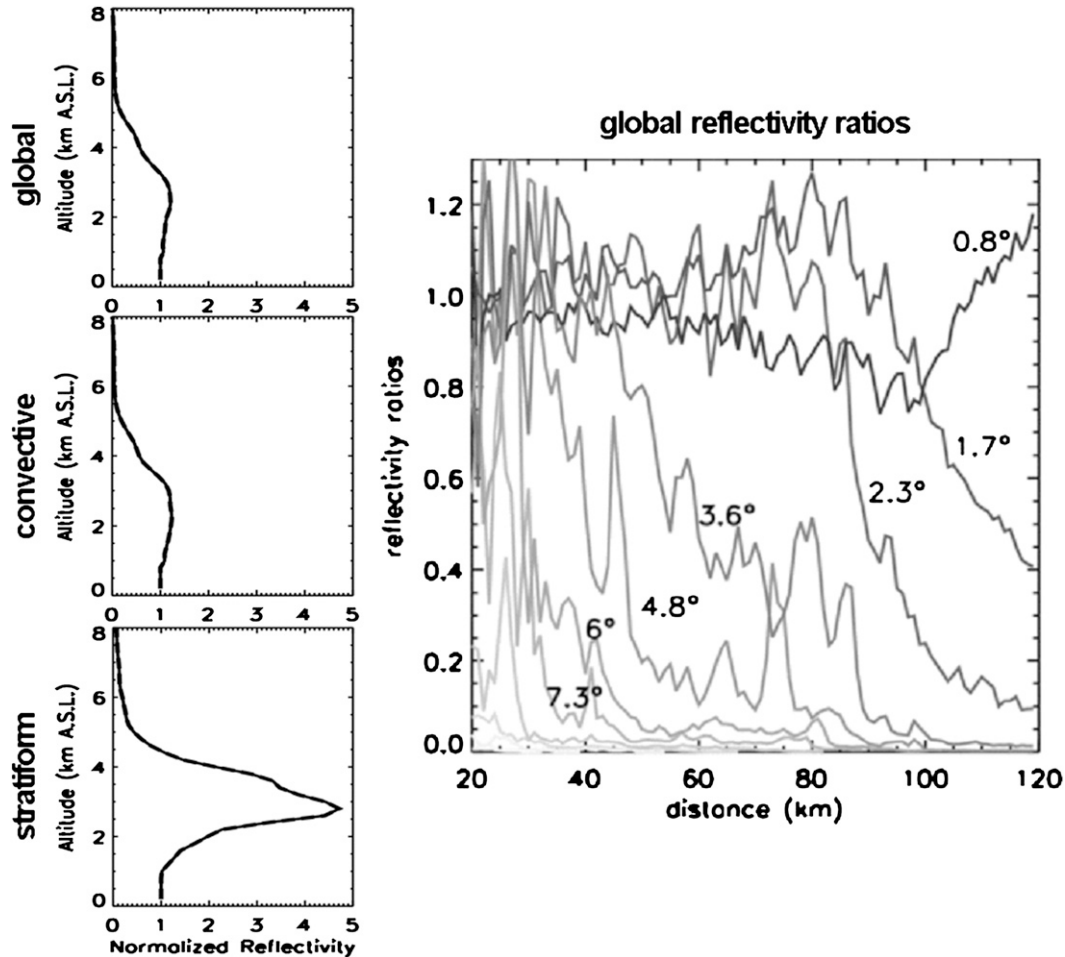


FIG. 3. (left) Apparent (a priori) VPR (top) for all the rainy pixels, (middle) for the convective pixels, and (bottom) for the stratiform pixels and (right) global reflectivity ratios computed from observations made between 0100 and 0200 UTC 9 Sep 2002. The corresponding upper-elevation angle is shown for each ratio curve. The apparent profiles have been established using reflectivity measurements within 60 km of the radar, whereas the reflectivity ratios used by the VPR inversion use reflectivity measurements up to 120 km from the radar.

before being handled by the VPR identification method, we avoid using measurements for which A_{ref} is significantly obstructed or is significantly contaminated by ground echoes. A space–time integration of the reflectivity at the two heights before the derivation of the ratio is applied. The requirement of the reflectivity at A_{ref} exceeding a certain threshold (12 dBZ) is imposed to reduce the probability of abnormally large ratios. Note that estimating the numerator and denominator of Eq. (6) strictly with the subset of $N(r, A_i, A_{\text{ref}})$ reflectivity observations available simultaneously for the two altitude classes $h_i(r, A_i)$ and $h_{\text{ref}}(r, A_{\text{ref}})$ at a given distance r within the same rain type region and over a 1-h period is an important condition to avoid biasing the reflectivity ratios.

After the time integration of the reflectivity-factor measurements at the two heights and given a distance and two elevation angles, numerous ratio values can be

calculated for different azimuth angles. From this population, a relative standard deviation associated with the average ratio value [using Eq. (6)] can be derived that characterizes the dispersion around the average value. The average value is the data for the VPR inverse method, and the standard deviation is accounted for in the data covariance matrix derivation.

For example, the ratio values calculated between 0100 and 0200 UTC 9 September are represented in Fig. 3. Relative to previous applications of the VPR identification method (e.g., Vignal et al. 1999), the variability of the measured ratios was found to be very high. These fluctuations, related to the high rainfall variability at short space–time scales and slanted trails of precipitation caused by vertical wind shear, are aggravated by several factors: 1) time-varying geographical domains are considered and therefore, for a given range and elevation angle pair, the

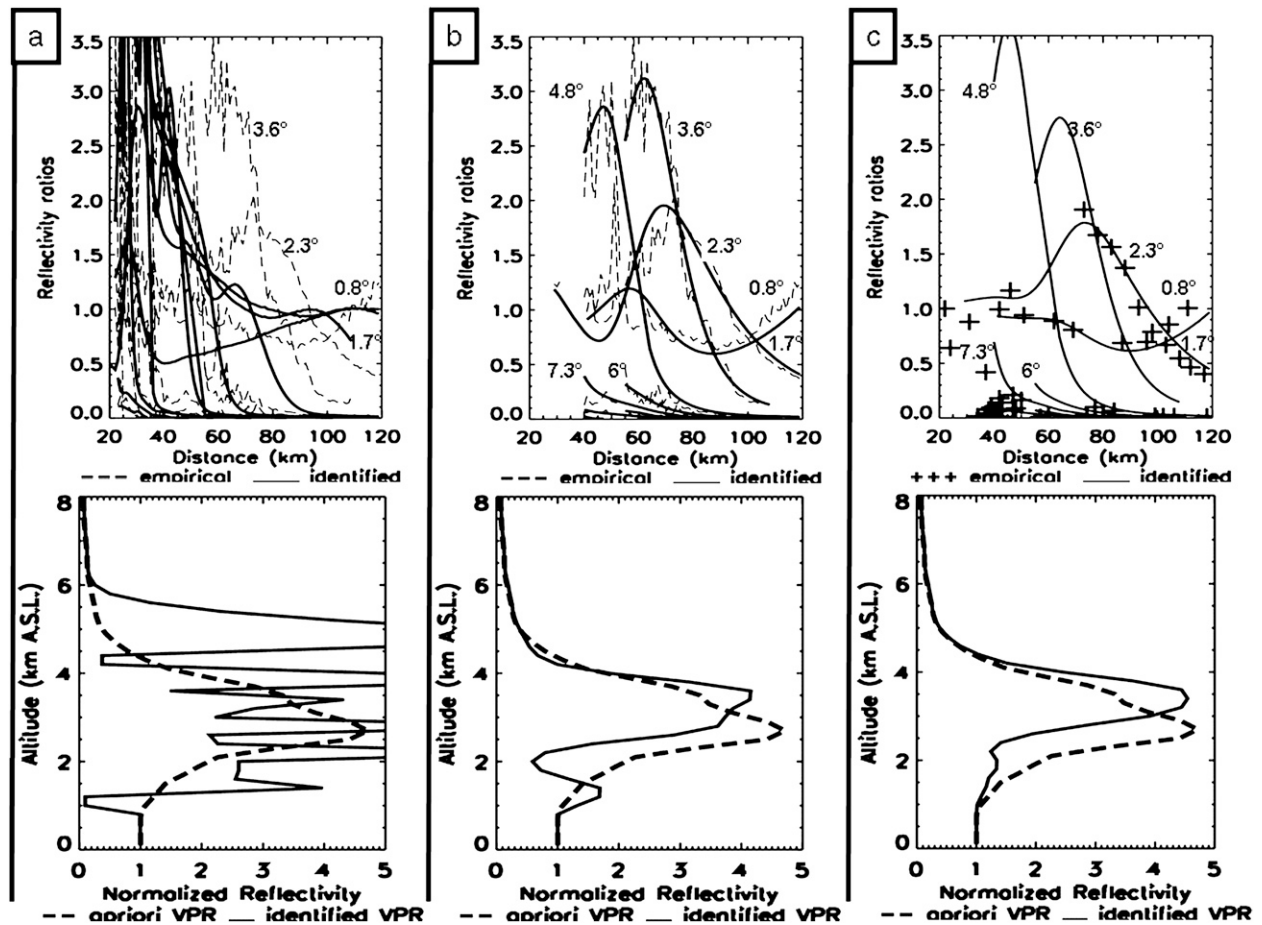


FIG. 4. Several identified stratiform VPRs computed by reflectivity ratio inversion from the observations made between 0100 and 0200 UTC (1 h). The performed inversions differ in terms of the data used: (a) all reflectivity ratios, (b) a sample of statistically more representative ratios (intermediate censoring), and (c) the minimum sample of representative ratios required to document each altitude class of the VPR (strong censoring). (top) Empirical reflectivity ratios [dashed gray lines in (a) and (b); crosses in (c)] and the ratios derived from the identified VPRs (black solid lines). The corresponding upper-elevation angle is shown for each ratio curve. (bottom) The a priori VPRs (dashed lines) and identified VPRs (solid lines).

ratios are established with reflectivity measurements that may come from different locations, 2) the observations for the numerator and denominator of Eq. (6) are not strictly synchronous, and 3) the VPR calculation is severely affected in the case of parasite detections, which are particularly strong for the considered wavelength and the considered mountainous and anthropogenic-influenced environment. The latter point puts the emphasis on the efficient correction of the parasite detections prior to the VPR identification.

Consideration of all of the computed ratios (as for fixed geographical domains) is not suitable in our case. Figure 4a illustrates for the stratiform case (the most affected by beam effects) the consequences of an inappropriate initialization stage, which results in an estimated VPR that is dramatically inconsistent with physical considerations. In this example, the presence of abnormal reflectivity ratios

(especially between 0 and 40 km) makes identification unstable. The representativeness of the experimental ratios was improved by means of a ratio data-censoring approach. Data censoring is based on the relative standard deviation of ratios, which gives an indication of the robustness and the representativeness of the ratio. A ratio value is assumed to be all the more representative of the vertical structure of reflectivity as its relative standard deviation decreases: in most cases, the ratios associated with lower robustness were found to correspond to the highest, and often spurious, values. Selecting the most statistically robust ratios seems therefore to be an efficient way to reduce the influence of the (unphysical) variability of the ratios. This approach can be used to select a necessary and sufficient subset to perform VPR identification. The ratio data-censoring approach is applied at the same space-time scale as the VPR identification (rain

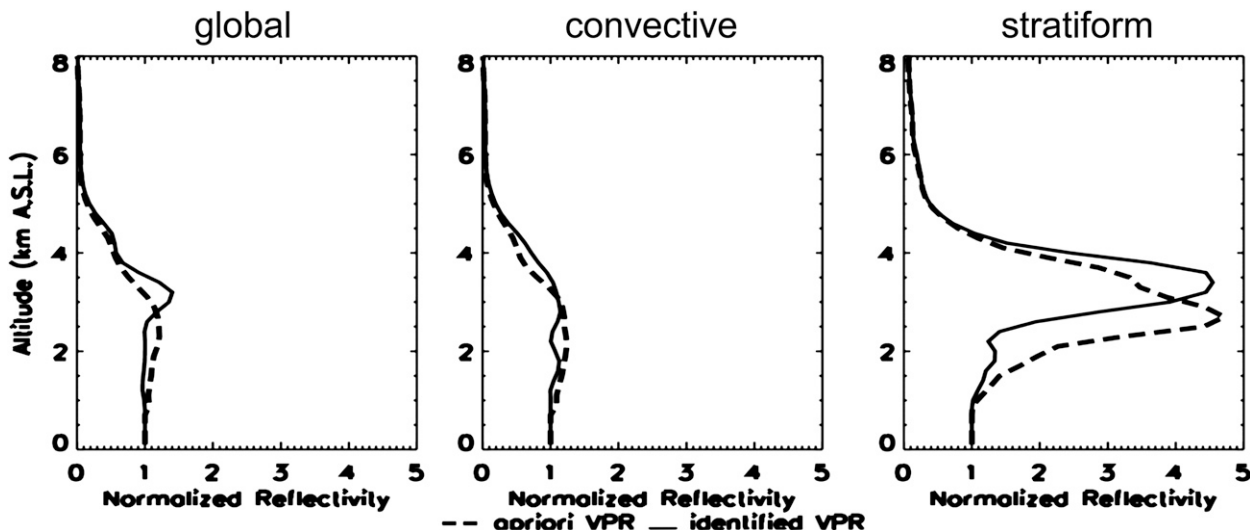


FIG. 5. A priori (dashed lines) and identified (solid lines) VPRs for the radar observations performed between 0100 and 0200 UTC 9 Sep 2002. The VPRs are computed from the most statistically representative ratios (high level of ratio censoring).

typed-1 h). For each range–height cell, we may dispose of several ratios, which are sorted by increasing relative standard deviation as an indication of their robustness. The highest level of censoring means retaining only one ratio (associated with the lowest relative standard deviation) by range–height cell to dispose of a sufficient dataset to perform the VPR identification. An intermediate level of censoring will retain, for example, two or more mean ratios by range–height cell if available.

Figures 4b and 4c illustrate the performance of the inversion for two levels of ratio censoring. In Fig. 4c, the highest level of censoring is considered with only one mean ratio value being retained for each altitude increment (90% of the total amount of original ratios have been eliminated). This subdataset of most representative reflectivity ratios is sufficient because it samples all of the VPR altitude components. An intermediate level of censoring is considered in Fig. 4b with 50% of the original ratios eliminated. Despite the radical nature of this approach, the highest level of censoring was found empirically to produce the most robust identification results, whereas, as seen in Fig. 4b, spurious oscillations of the identified VPR reflect the difficulty the inversion method encounters in attempting to produce a coherent synthesis of the data for the intermediate level of ratio censoring. In summary, data censoring makes it possible to select representative ratios of reflectivity, thereby improving the robustness of VPR identification.

5. Results

The VPR identification method identifies hourly VPRs associated with rain types. It is initialized by a priori VPRs

directly derived from measured reflectivity data in the vicinity of the radar site. The inversion method is assessed by evaluating the improvement achieved with respect to this first estimate. This can be done in three different ways: 1) by using a qualitative approach that consists of verifying that the obtained VPRs display better characteristics than the corresponding apparent VPRs, 2) by checking that the identified VPRs better reproduce the reflectivity ratios than the a priori VPRs (note that the reflectivity ratios are the signature of the actual VPRs, as seen by the radar), and 3) by checking that identified VPRs improve rainfall estimation in comparison with correction based on climatological VPR or apparent VPR.

As an illustration, the results obtained for the example of 0200 UTC 9 September 2002 are displayed in Fig. 5. Comparison of the a priori and the identified VPR shows the effects of the VPR identification method. As expected, the convective-identified VPR is close to the apparent VPR but the stratiform-identified VPR presents a finer and higher bright band, consistent with simulations of beamwidth-smoothing effects (Sanchez-Diezma et al. 2000). Note that the stratiform-identified VPR presents still a large bright band relative to values mentioned in the literature from vertically pointing radar observations (e.g., Fabry and Zawadzki 1995). This behavior can most likely be explained by the observation conditions (slant elevation angles) and the spatial variations of the bright band within the domain of interest: the identified stratiform VPR shows the mean features of the stratiform VPR population. Nevertheless, the identified bright band is half as thick as the apparent one. The proposed approach therefore corrects a significant amount of the radar

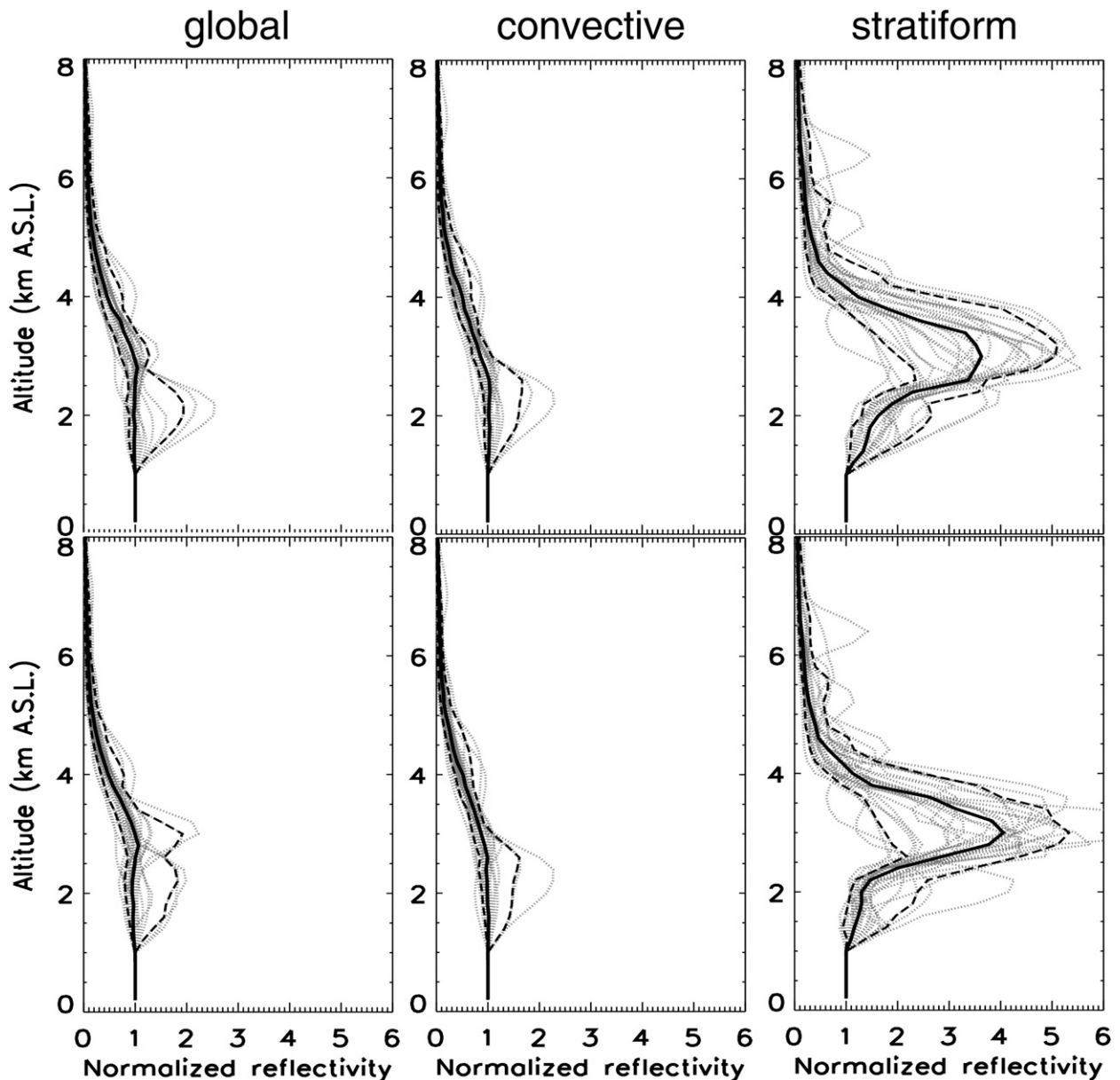


FIG. 6. Hourly (top) a priori and (bottom) identified (considering the most representative reflectivity ratios) VPRs (gray curves) for the 8–9 Sep 2002 rainfall event. (left) Global estimation without rain classification, and estimations for the (center) convective and (right) stratiform regions. The 10%, 50%, and 90% quantiles of the distribution are displayed with dotted and solid black lines.

beam-smoothing effects. The identified VPR for all of the rainy pixels (referred to as “global” in Fig. 5) exhibits a small bright band and lies somewhere between the convective- and stratiform-identified VPRs. Note that because there are about 2 times more stratiform pixels than convective pixels within the 120-km range one would expect a bigger brightband effect for the global VPR. However, both the algorithms for the apparent and identified VPR estimation favor the information that is less affected (smoothed) by the beam effects, that is, that

comes from near ranges. Figure 1 clearly shows that the convective pixels are dominant close to the radar, which explains the observed behavior.

As a generalization of this specific case, Fig. 6 shows the apparent and identified VPR distributions for the successive hours of the 8–9 September 2002 event. For the median profiles, the qualitative improvements (thinner and higher bright band) are confirmed for the event VPR population. This confirms the robustness of the proposed approach in dealing with various conditions of sampling

of the radar and typed VPR identification on a more representative region than the apparent VPR.

The effectiveness of the VPR identification method may also be assessed by testing its ability to reproduce the experimental reflectivity ratios, which are representative of the reflectivity field. The Nash–Sutcliffe criterion may be computed between the experimental ratios and those that can be derived from both the apparent and identified VPRs for each hourly time step. These criterion values may then be sorted in increasing order to compute a so-called efficiency curve (Creutin and Obled 1982), equivalent to the distribution function of this criterion. The closer the efficiency curve is to the horizontal line at 1, the better is the tested method. To compare the different methods fairly, the validation dataset must be different from the one used for fitting. The empirical ratio samples retained as a reference for the calculation of the criteria are 2 times as numerous as the samples retained for VPR identification (e.g., empirical ratios sample of Fig. 4b). The performance assessment of VPR identification is illustrated in Fig. 7. In comparing the a priori VPR with the identified VPR, it clearly appears that the identified VPRs better reproduce the observed ratios than the a priori VPRs. The best improvements are obtained for the stratiform case, which somewhat compensates for the moderate ratio reproduction from the apparent stratiform VPR; improvements are less marked in the convective case (where room for improvement is lower) and are moderate in the global case. The VPR identification method therefore provides VPRs that are more representative of the reflectivity field over a larger region (within a radar range of 120 km, as compared with an area extending over a 60-km range for the apparent VPR estimation).

Last, an indirect means to evaluate the effectiveness of VPR identification may be to quantify the contribution of the identified VPR in radar data processing. By comparing the radar QPE with a reference rainfall on the ground, it is possible to check whether this identification improves the radar rainfall estimation. We expand hereinafter the assessment results presented in Delrieu et al. (2009) to highlight the relative performance of the VPR identification method with respect to the apparent VPRs. We simply recall here that five intense rain events observed during the autumn of 2002 were considered in such assessment, globally and for 3 groups of events corresponding to an extreme MCS (28 h), two frontal events (total of 32 h), and two shallow convective events (total of 116 h). We restrict the following analyses to the case of the processing strategy that includes rain classification and the use of the apparent or identified VPRs and of two predefined radar reflectivity–rainfall (Z – R) relationships for the convective type ($Z = 300R^{1.4}$) and the other rain

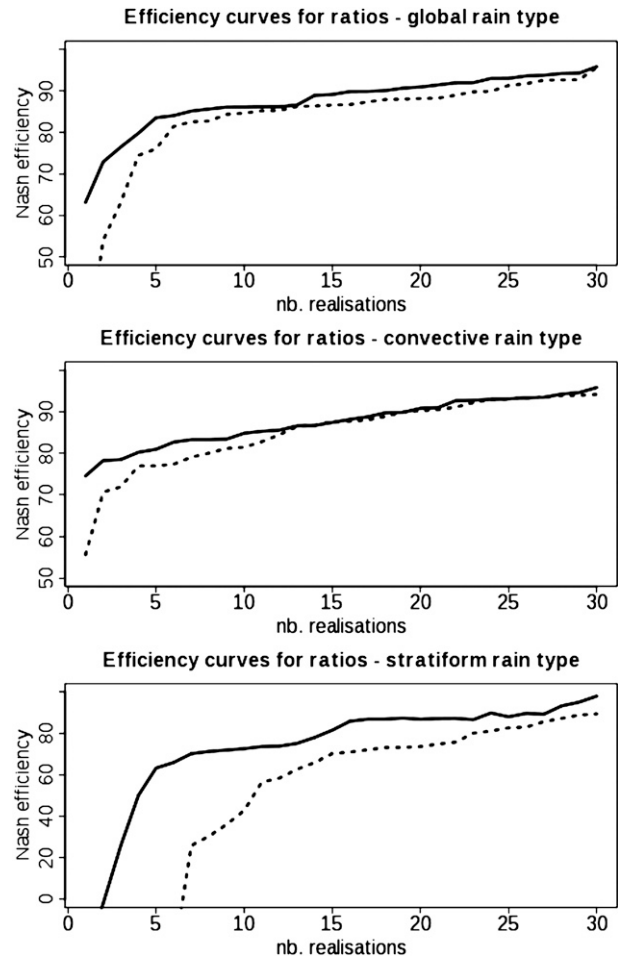


FIG. 7. Efficiency curves of the Nash–Sutcliffe criterion for hourly apparent VPRs (dashed curves) and identified VPRs with the most representative ratios (solid curves) for (top) all of the rainy pixels, (middle) convective pixels, and (bottom) stratiform pixels during the 8–9 Sep 2002 event.

types ($Z = 200R^{1.6}$). Table 1 lists the assessment criteria with 1) the mean relative error [$MRE = (\bar{R} - \bar{G})/\bar{G}$, where \bar{G} and \bar{R} stand for rain gauge and radar mean rain amounts, respectively], 2) the mean absolute difference ($MAD = |\bar{R} - \bar{G}|/\bar{G}$), and 3) the determination coefficient (square of the linear correlation coefficient). The overall level of radar–rain gauge agreement is high at the event time step (determination coefficient of about 0.9), and it remains relatively good at the hourly time step (determination coefficient of 0.76). The scatter naturally increases as the time scale decreases. The MRE is significantly reduced for identified VPRs relative to that of apparent VPRs, and both the MAD and the determination coefficient are almost unchanged. Table 1 indicates that this overall trend remains the same for the three groups of events whereas performance varies with the group of events. For the MCS case, the stratiform part

TABLE 1. Assessment criteria for different rain event groups at hourly and event time steps.

	No. hours	No. pairs	Apparent VPR			Identified VPR		
			MRE (%)	MAD (%)	ρ^2	MRE (%)	MAD (%)	ρ^2
Assessment at the hourly time step								
All events	176	24868	-6	46	0.76	0	49	0.74
MCS event	28	6395	-9	40	0.80	-6	38	0.80
Frontal events	32	5979	-10	44	0.76	-4	45	0.77
Shallow convective events	116	12239	-1	54	0.56	10	59	0.51
Assessment at the event time step								
All events	176	1240	-12	25	0.90	-7	25	0.89
MCS event	28	249	-13	20	0.92	-9	19	0.92
Frontal events	32	498	-16	25	0.71	-11	24	0.71
Shallow convective events	116	498	-19	33	0.76	-10	33	0.71

of the system generated a much smaller contribution in terms of rainfall than the convective part. In addition, the location of the event at close range of the radar and the high altitude of the bright band (3.2 km) also explain the limited influence of the VPR correction. In that specific case, the choice of the (convective) $Z-R$ relationship was certainly a more critical issue in terms of QPE. There is still a positive though moderate impact of the identified VPRs relative to the apparent VPRs in terms of bias reduction; of interest is that the MAD is also significantly improved while the determination coefficient is unchanged for both time steps. For the rain events associated with cold-frontal systems, there is a more significant improvement in terms of MRE reduction. As noted in Delrieu et al. (2009), the performance for the shallow convective events is poor because of the observation conditions in that mountainous part of the region. In summary, the use of identified VPRs has a positive and very systematic impact in terms of bias reduction in comparison with the use of apparent VPRs, whereas the scatter remains unchanged or slightly altered. This result is attributed to the better processing of spatial variations of the vertical profile of reflectivity for the stratiform regions. This statement is supported by the MRE reduction at the event time scale while the determination coefficient remains basically unchanged, as an indication of the better processing of the low rain rates (stratiform) while the high rain rates (convection) are not significantly changed.

6. Conclusions

This note has proposed improvements to the VPR identification algorithm proposed by Vignal et al. (1999) based on inversion of reflectivity ratios computed over the distance from the radar. VPR identification is a valuable approach to synthesize radar data that provide heterogeneous information on the VPR, being differently affected by the range influence. It complements and improves methods that directly derive VPRs from measured

reflectivity data (Germann and Joss 2002; Delrieu et al. 2009). The improvements of the method concern 1) the use of a range-weighted apparent VPR as a first guess of the VPR identification, 2) the application of the VPR identification method to time-varying geographic domains in which the type of precipitation is homogeneous, and 3) the selection of the most representative data (reflectivity ratios) to perform the VPR identification.

The study of the spatial variations of VPRs made it possible to better define the application conditions of the proposed method. By aggregating typed rain data over 1 h, we expect to define domains over which the vertical structure of reflectivity will show a relative prior homogeneity. The apparent VPR used to initialize the method may be considered to be a well-designed prior estimator, in comparison with which the inverse method is a refined homogenization.

The applicability of this VPR identification method has been tested in the difficult context of intense rain events where a reliable evaluation of rainfall is a major issue for flood warning. Despite the fact that the VPR homogeneity assumption is more fully satisfied using the rain separation algorithm, adapting the inversion technique to the case of variable geographic domains still proved challenging relative to previous implementations based on fixed spatial domains (Andrieu et al. 1995; Vignal et al. 1999, 2000; Vignal and Krajewski 2001). Two conditions ultimately allowed for robust inversions to be achieved: 1) aggregating data from several successive (1 h) time steps and 2) implementing a ratio data-censoring approach.

Positive results have been obtained, insofar as the identified VPR 1) qualitatively presents physically consistent shapes and better characteristics than the apparent VPR considering beam effects, 2) better reproduces the reflectivity ratio curves, which are representative of the reflectivity field and represent the radar signature of the actual VPR, and 3) has a positive impact on radar data processing for quantitative precipitation estimation

in terms of bias reduction. The identification method is efficient to correct for the beam effect's smoothing on VPR shape; it is all the more significant in the presence of strong vertical gradients in the VPR shape, as for the stratiform type.

However, given the variability of the ratios in the difficult radar measurement context of the Cévennes–Vivarais region, it would appear that the limits of this VPR identification method have been reached. As the VPR identification is based on the key assumption of spatial homogeneity of the VPR, these fluctuations are liable to make the VPR identification unstable and prevent its application. Moreover the method is based on statistical control of the variations of the VPR components about their a priori values, and in the case of strong and possibly abnormal fluctuations of the observed data this statistical control is not sufficiently robust to prevent identified VPRs that are unrealistic from a physical point of view. A more promising approach would be to replace the statistical control of the VPR about its a priori value by the introduction of physically based constraints into the inverse algorithm to identify a more physically shaped VPR. This approach will be the subject of an upcoming paper.

Acknowledgments. The critical comments of two anonymous reviewers were very helpful to improving the manuscript. This study was funded by the HYDRATE project (GOCE-STREP-037024, FP6) of the European Community.

REFERENCES

- Andrieu, H., and J. D. Creutin, 1995: Identification of vertical profiles of radar reflectivity using an inverse method. Part I: Formulation. *J. Appl. Meteor.*, **34**, 225–239.
- , G. Delrieu, and J. D. Creutin, 1995: Identification of vertical profiles of radar reflectivity using an inverse method. Part II: Sensitivity analysis and case study. *J. Appl. Meteor.*, **34**, 240–259.
- Bellon, A., G. W. Lee, and I. Zawadzki, 2005: Error statistics of VPR corrections in stratiform precipitation. *J. Appl. Meteor.*, **44**, 998–1015.
- , —, A. Kilambi, and I. Zawadzki, 2007: Real-time comparisons of VPR-corrected daily rainfall estimates with a gauge mesonet. *J. Appl. Meteor. Climatol.*, **46**, 726–741.
- Berne, A., G. Delrieu, H. Andrieu, and J.-D. Creutin, 2004: Influence of the vertical profile of reflectivity on radar-estimated rain rates at short time steps. *J. Hydrometeorol.*, **5**, 296–310.
- Bonnifait, L., G. Delrieu, M. Le Lay, B. Boudevillain, A. Masson, P. Belleudy, E. Gaume, and G. M. Saulnier, 2009: Hydrologic and hydraulic distributed modeling with radar rainfall input: Reconstruction of the 8–9 September 2002 catastrophic flood event in the Gard region, France. *Adv. Water Resour.*, **32**, 1077–1089.
- Boudevillain, B., and H. Andrieu, 2003: Assessment of vertically integrated liquid (VIL) water content radar measurement. *J. Atmos. Oceanic Technol.*, **20**, 807–819.
- Creutin, J.-D., and C. Obled, 1982: Objective analyses and mapping techniques for rainfall fields: An objective comparison. *Water Resour. Res.*, **18**, 413–431.
- Delrieu, G., and Coauthors, 2005: The catastrophic flash-flood event of 8–9 September 2002 in the Gard region, France: A first case study for the Cévennes–Vivarais Mediterranean Hydrometeorological Observatory. *J. Hydrometeorol.*, **6**, 34–52.
- , B. Boudevillain, J. Nicol, B. Chapon, P.-E. Kirstetter, H. Andrieu, and D. Faure, 2009: Bollène 2002 experiment: Radar rainfall estimation in the Cévennes–Vivarais region. *J. Appl. Meteor. Climatol.*, **48**, 1422–1447.
- Fabry, F., and I. Zawadzki, 1995: Long-term radar observations of the melting layer of precipitation and their interpretation. *J. Atmos. Sci.*, **52**, 838–851.
- Germann, U., and J. Joss, 2002: Mesobeta profiles to extrapolate radar precipitation measurements above the Alps to the ground level. *J. Appl. Meteor.*, **41**, 542–557.
- , G. Galli, M. Boscacci, and M. Bolliger, 2006: Radar precipitation measurement in a mountainous region. *Quart. J. Roy. Meteor. Soc.*, **132**, 1669–1692.
- Gourley, J. J., and C. M. Calvert, 2003: Automated detection of the bright band using WSR-88D data. *Wea. Forecasting*, **18**, 585–599.
- Harrison, D. L., S. J. Driscoll, and M. Kitchen, 2000: Improving precipitation estimates from weather radar using quality control and correction techniques. *Meteor. Appl.*, **7**, 135–144.
- Joss, J., and R. Lee, 1995: The application of radar-gauge comparisons to operational precipitation profile corrections. *J. Appl. Meteor.*, **34**, 2612–2630.
- Kirstetter, P.-E., 2008: Estimation quantitative des précipitations par radar météorologique: inférence de la structure verticale des pluies et modélisation des erreurs radar-pluviomètres (Radar quantitative precipitation estimation: inference of the vertical profile of reflectivity, radar-rain gauge error model). Ph.D. thesis, University Joseph Fourier, Grenoble, France, 210 pp.
- Kitchen, M., R. Brown, and A. G. Davies, 1994: Real-time correction of weather radar data for the effects of bright band, range and orographic growth in widespread precipitation. *Quart. J. Roy. Meteor. Soc.*, **120**, 1231–1254.
- Marzano, F. S., G. Vulpiani, and E. Picciotti, 2004: Rain field and reflectivity vertical profile reconstruction from C-band radar volumetric data. *IEEE Trans. Geosci. Remote Sens.*, **42**, 1033–1046.
- Matrosov, S. Y., K. A. Clark, and D. E. Kingsmill, 2007: A polarimetric radar to identify rain, melting-layer and snow regions for applying corrections to vertical profiles of reflectivity. *J. Appl. Meteor. Climatol.*, **46**, 154–166.
- Menke, W., 1989: *Geophysical Data Analysis: Discrete Inverse Theory*. Academic Press, 260 pp.
- Pellarin, T., G. Delrieu, G. M. Saulnier, H. Andrieu, B. Vignal, and J. D. Creutin, 2002: Hydrologic visibility of weather radars operating in mountainous regions: Case study for the Ardèche catchment (France). *J. Hydrometeorol.*, **3**, 539–555.
- Sanchez-Diezma, R., I. Zawadzki, and D. Sempere-Torres, 2000: Identification of the bright band through the analysis of volumetric radar data. *J. Geophys. Res.*, **105**, 2225–2236.
- Seo, D.-J., J. P. Breidenbach, R. A. Fulton, D. A. Miller, and T. O'Bannon, 2000: Real-time adjustment of range-dependent bias in WSR-88D rainfall data due to nonuniform vertical profile of reflectivity. *J. Hydrometeorol.*, **1**, 222–240.

- Steiner, M., R. A. Houze Jr., and S. E. Yuter, 1995: Climatological characterization of three-dimensional storm structure from operational radar and rain gauge data. *J. Appl. Meteor.*, **34**, 1978–2007.
- Tabary, P., 2007: The new French operational radar rainfall product. Part I: Methodology. *Wea. Forecasting*, **22**, 393–408.
- , J. Desplats, K. Do Khac, F. Eideliman, C. Gueguen, and J.-C. Heinrich, 2007: The new French operational radar rainfall product. Part II: Validation. *Wea. Forecasting*, **22**, 409–427.
- Vignal, B., and W. F. Krajewski, 2001: Large-sample evaluation of two methods to correct range-dependent error for WSR-88D rainfall estimates. *J. Hydrometeorol.*, **2**, 490–504.
- , H. Andrieu, and J. D. Creutin, 1999: Identification of vertical profiles of reflectivity from volume scan radar data. *J. Appl. Meteor.*, **38**, 1214–1228.
- , G. Galli, J. Joss, and U. Germann, 2000: Three methods to determine profiles of reflectivity from volumetric radar data to correct precipitation estimates. *J. Appl. Meteor.*, **39**, 1715–1726.
- Zawadzki, I., W. Szyrmer, C. Bell, and F. Fabry, 2005: Modeling of the melting layer. Part III: The density effect. *J. Atmos. Sci.*, **62**, 3705–3723.
- Zhang, J., C. Langston, and K. Howard, 2008: Brightband identification based on vertical profiles of reflectivity from the WSR-88D. *J. Atmos. Oceanic Technol.*, **25**, 1859–1872.